

QUANTUM CHEMICAL STUDIES OF CHITOSAN NANOPARTICLES AS ANTICANCER DRUG DELIVERY SYSTEM FOR DECITABINE

MAHNAZ RAHBAR,* ALI MORSALI,** MOHAMMAD REZA BOZORGMEHR* and S. ALI BEYRMABADI*

*Department of Chemistry, Mashhad Branch, Islamic Azad University, Mashhad, Iran

**Research Center for Animal Development Applied Biology, Mashhad Branch, Islamic Azad University, Mashhad 917568, Iran

✉ Corresponding author: A. Morsali, morsali@mshdiau.ac.ir

Received February 2, 2020

Applying DFT functionals (B3LYP and M06-2X), ten structures for the adsorption of decitabine medicine (DC) onto a chitosan nanocarrier (CHIT) were studied. The solvation and binding energies were evaluated in solution (water) and gas phases. Here, we used the negative values of binding energies to represent the energetic stability of ten structures (CHIT/DC1-10). The solvation energies showed that the solubility of DC drug increased near the CHIT nanocarrier and thus it could be a main element for the applicability of any nanocarrier. Here, the quantum molecular descriptors revealed that the toxicity of DC in ten structures was reduced to some extent and its own reactivity increased. Analyzing the data obtained by the Atoms in Molecules (AIM) method for CHIT/DC1-10, it has been found that the hydrogen bonds are an essential element in the non-covalent functionalization of CHIT with DC.

Keywords: chitosan, decitabine, nanocarrier, DFT, Schiff base, decitabine drug, hydrogen bonds

INTRODUCTION

For decreasing the issues of anticancer drugs, such as low selectivity, high toxicity, side effects, water insolubility and poor stability, many studies have already been conducted on drug delivery systems. Many of these studies have been carried out on carbon-based nanocarrier systems, like carbon nanotubes,¹⁻⁵ dendrimers,⁶ liposomes,⁷ drug-polymer conjugates,⁸ C60 and chitosan.⁹⁻¹⁰ Chitosan is a good drug carrier obtained from the chitin polysaccharide.

Nanostructures of chitosan (chitosan nanoparticles) have already been applied in drug delivery systems due to their properties, such as biocompatibility, non-toxicity, high permeability, renewability, solubility in mild acid, low allergenicity, and biodegradability of surface functional groups (NH₂ and OH).¹¹⁻¹⁶ Chitosan has many properties that are linked to its primary amine group, including hydrogen bond formation, muco-adhesion, cationic nature, controlled drug release, antimicrobial activity, and permeation enhancement.^{11,12} Different forms of chitosan and its derivatives have been used as gels, films, fibers, beads, solutions and powder.¹⁰

Chitosan nanoparticles have been successfully used as carrier molecules as they demonstrated that lower doses of anticancer drugs are sufficient, thus decreasing their side effects. Thus, chitosan has been used as carrier for various anticancer drugs, such as decitabine,¹⁸⁻²¹ doxorubicin,²¹⁻²³ cisplatin,^{24,25} nifedipine,^{26,27} methotrexate,^{27,28} melphalan,²⁹ paclitaxel,^{30,31} artemisinin,³² 10-hydroxycamptothecin,³³ capecitabine,³⁴ etoposide,³⁵ gemcitabine,^{36,37} and mercaptopurine.³⁸ In addition, chitosan has been also reported as drug carrier for Alzheimer's illness,³⁹ HIV,^{40,41} inflammation⁴² and bacteria.⁴³

We used quantum computing since it is a really powerful tool for analyzing drug delivery systems.⁴⁴⁻⁴⁷ In this article, we used quantum chemical calculations to review non-covalent functionalization of chitosan with decitabine. Researchers can benefit from the results to develop and apply targeted anticancer drugs and shorten the trial-and-error process in the lab. Moreover, decitabine (trade name Dacogen), or 5-aza-2-deoxycytidine, could act as a nucleic acid synthesis inhibitor. This is a drug for treatment of

myelodysplastic syndromes, a category of situations where certain blood cells are dysfunctional, as well as for acute myeloid leukemia.

EXPERIMENTAL

Computational method

In this paper, the GAUSSIAN 09 package⁴⁸ was applied to optimize the key structures in gas phase and solution phase at M06-2X⁴⁹/6-31G(d,p)⁵⁰ and B3LYP⁵¹/6-31G(d,p) levels of theory. Considering the implicit solvent effects, the polarized continuum model (PCM) was utilized.^{52,53} In addition, we used the standard convergence criteria for optimization of the molecular structures. For all species, we optimized the degrees of freedom. Furthermore, we considered zero-point corrections. Having only one imaginary frequency of the Hessian, we examined these transition states.

Quantum molecular descriptors enable examining chemical reactivity and stability; η as global hardness represents the resistance of one particle against the modification in its electronic structure:

$$\eta = (I - A)/2 \quad (1)$$

in which $I = -E_{HOMO}$ and $A = -E_{LUMO}$ are the ionization potential and the electron affinity, respectively. The electrophilicity index (ω)⁵⁴ can be evaluated by:

$$\omega = (I + A)^2/8\eta \quad (2)$$

We used the QTAIM (Quantum Theory of Atoms in Molecules) calculations to study the hydrogen bond. AIMAll software⁵⁵ was applied for QTAIM calculations. Topological parameters as electron density $\rho(r)$ ⁵⁶ were used in QTAIM. The nature of the bonds in various species was identified to analyze various values of electron density, such as V_b (potential energy density), G_b (kinetic energy density), $\nabla^2\rho$ (Laplacian of electron density) and H_b (total energy density) at a bond critical point (BCP).

RESULTS AND DISCUSSION

Using a polymer sequence with 3 monomer units, chitosan nanoparticles were modeled. The optimized configuration of the chitosan nanoparticle (CHIT) and decitabine (DC) are presented in Figure 1. The interaction of decitabine, which consists of one CO, one NH₂, two OH, one O and three N functional groups, with the chitosan nanoparticle has been evaluated for ten different structures (CHIT/DC1-10). The optimized configurations of CHIT/DC1-5 and CHIT/DC5-10 are illustrated in Figures 2 and 3, respectively (in aqueous solution at M06-2X/6-31G (d, p) level of theory).

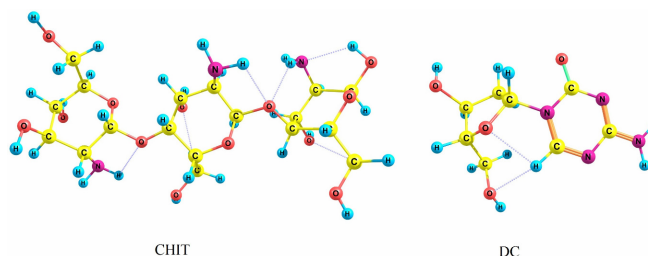


Figure 1: Optimized structures of DC and CHIT

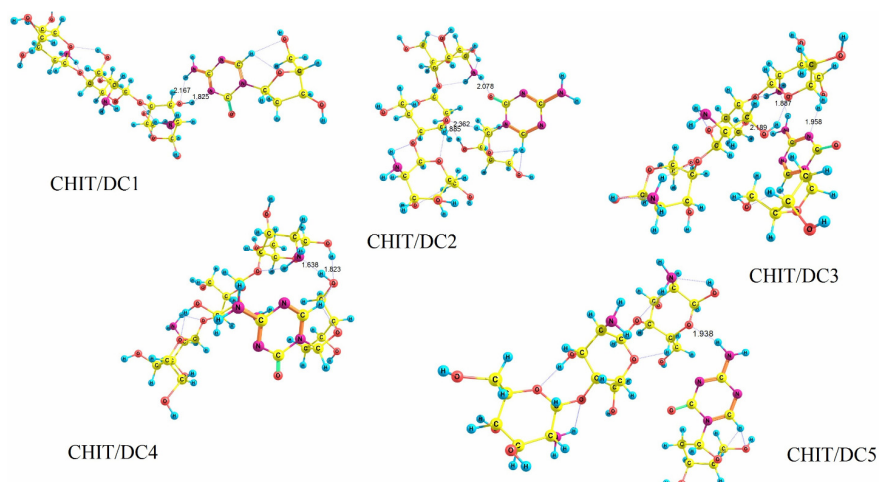


Figure 2: Optimized structures of CHIT/DC1-5

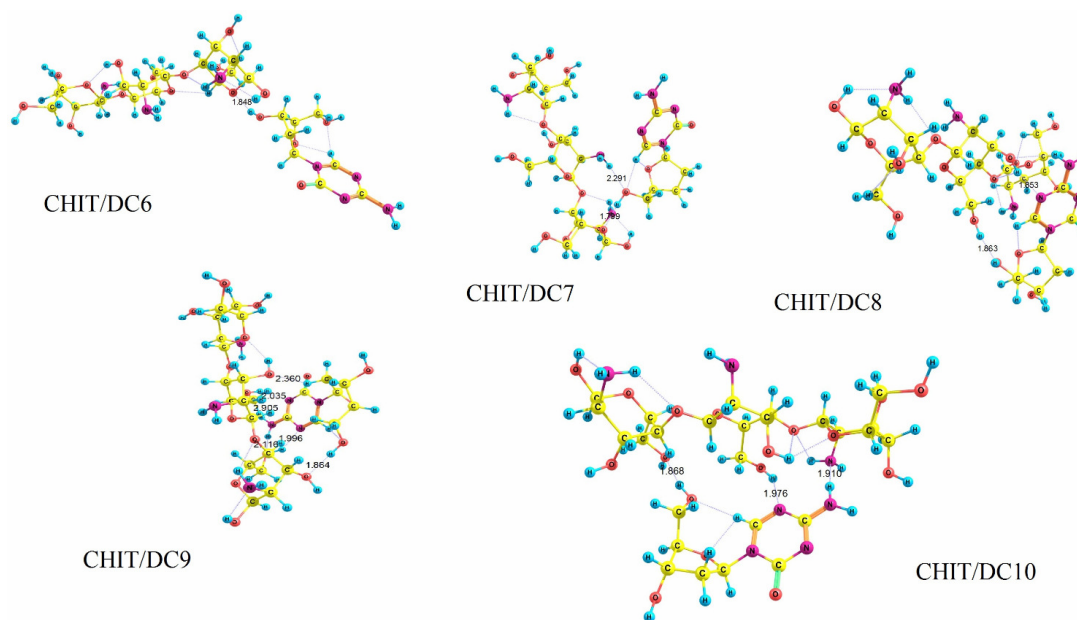


Figure 3: Optimized structures of CHIT/DC6-10

Table 1
Binding (ΔE) and solvation (ΔE_{solv}) energies (kJ mol^{-1}) for optimized geometries

Species	$\Delta E_{\text{solv}}^{\text{B3LYP}}$	$\Delta E_{\text{solv}}^{\text{M06-2X}}$	$\Delta E_{\text{gas}}^{\text{B3LYP}}$	$\Delta E_{\text{gas}}^{\text{M06-2X}}$	$\Delta E_{\text{gas}}^{\text{B3LYP}}$	$\Delta E_{\text{gas}}^{\text{M06-2X}}$
DC	-65.8	-67.3	-	-	-	-
CHIT	-87.9	-85.8	-	-	-	-
CHIT/DC1	-153.5	-159.6	-56.0	-55.8	-66.2	-72.8
CHIT/DC2	-148.5	-120.5	-65.5	-60.3	-130.5	-98.0
CHIT/DC3	-118.7	-127.4	-106.8	-71.8	-152.5	-126.9
CHIT/DC4	-149.0	-87.9	-75.0	-70.3	-154.9	-89.7
CHIT/DC5	-149.4	-84.5	-47.5	-43.2	-129.1	-60.5
CHIT/DC6	-138.7	-162.9	-60.9	-45.8	-53.9	-63.7
CHIT/DC7	-148.1	-157.8	-61.5	-55.9	-74.5	-79.2
CHIT/DC8	-165.8	-137.2	-68.6	-80.7	-125.2	-109.4
CHIT/DC9	-142.9	-115.9	-83.2	-72.4	-144.6	-107.5
CHIT/DC10	-145.7	-117.4	-93.9	-85.8	-163.0	-127.3

Interaction (binding) energies (ΔE) for CHIT/DC1-10 structures were calculated using the following equation:

$$\Delta E = E_{\text{CHIT/DC1-10}} - (E_{\text{CHIT}} + E_{\text{DC}}) \quad (3)$$

Table 1 shows the ΔE values at both levels of B3LYP and M06-2X in aqueous solution and gas phase. The ΔE values calculated by M06-2X functional are more negative than those of B3LYP. Unlike B3LYP, dispersion corrections⁵⁷ are considered by M06-2X functional; therefore, these interactions (dispersion corrections) emerge as interesting forces. The ΔE s in gas phase (-

119.44 kJ mol^{-1} and -71.89 kJ mol^{-1} on average at M06-2X and B3LYP, respectively) are more negative than those in aqueous solution (-93.5 kJ mol^{-1} and -64.2 kJ mol^{-1} on average at M06-2X and B3LYP, respectively) because the solvent molecules compete with the drug molecules for adsorption. On the other hand, the interaction energies are negative for both functionals, showing that the surface adsorption of the decitabine drug onto the chitosan carrier is good.

The ΔE s were determined by the orientation of decitabine in accordance with the adsorbent. Based on the results obtained by both B3LYP and

M06-2X functionals, among the 10 different structures, CHIT/DC10 has the most negative connection energy in aqueous solution (probably the most stable one), where the NH_2 and N functional groups of DC interact with the NH_2 and OH functional groups of CHIT, respectively (Fig. 3). Concerning stability, the CHIT/DC3 structure is positioned as the second one in aqueous solution. The range of binding energy values is in agreement with the values obtained from the interaction of chitosan with other biological and therapeutic agents.⁵⁸⁻⁶⁰ Due to the large negative ΔE s, it is predicted that sufficient drug loading will be achieved.⁶¹⁻⁶³

The solvation energies (ΔE_{solv}) were evaluated using the following equation (Table 1):

$$\Delta E_{\text{solv}} = E_{\text{aq}} - E_{\text{gas}} \quad (4)$$

where E_{gas} and E_{aq} show the energies (sum of electronic and zero-point energies) in the gas phase and solution phase, respectively.

An appropriate carrier for a specific drug should increase the solubility of the drug in aqueous solution. The ΔE_{solv} of DC ($-67.3 \text{ kJ mol}^{-1}$ and $-65.8 \text{ kJ mol}^{-1}$ at M06-2X and B3LYP, respectively) becomes more negative in the current presence of chitosan ($-127.1 \text{ kJ mol}^{-1}$ and $-146.0 \text{ kJ mol}^{-1}$ on average at M06-2X and B3LYP, respectively), so the solubility of DC is increased by CHIT. The primary reason for the increase in solubility and strong interactions relates to the forming of hydrogen bonds between the drug and the carrier, which is discussed in

detail within the next part by the quantum theory of atoms in molecules. Considering the intermolecular hydrogen bonds more closely, charge density properties are used. The interactions were evaluated by QTAIM research. The character and strength of an interaction could be displayed by $\nabla^2 \rho(r)$ and $\rho(r)$, respectively. Nevertheless, the signs of $\nabla^2 \rho$ and H_b present the nature of the interactions. If, $(\nabla^2 \rho > 0, H_b > 0)$, $(\nabla^2 \rho > 0, H_b < 0)$ and $(\nabla^2 \rho < 0, H_b < 0)$, then weak, medium and strong interactions are expected, respectively.⁶⁴ The character of an interaction can be defined by $-G_b/V_b$. For $-G_b/V_b > 1$ and $0.5 < -G_b/V_b < 1$, non-covalent and partially covalent characters are predicted, respectively.

The molecular graphs of CHIT/DC1-5 and CHIT/DC 6-10 in aqueous solution at M06-2X/6-31G** level of theory are shown in Figures 4 and 5, respectively. The atoms participating in the interactions will be marked in the figures. The $\rho(r)$, $\nabla^2 \rho(r)$, H_b , G_b , V_b and $-G_b/V_b$ values for these interactions are displayed in Table 2 (at M06-2X/6-31G** level of theory in aqueous solution). The hydrogen bond energy (E_{HB}) continues to be approximated by the following equation:

$$E_{\text{HB}} = \frac{V_b}{2} \quad (5)$$

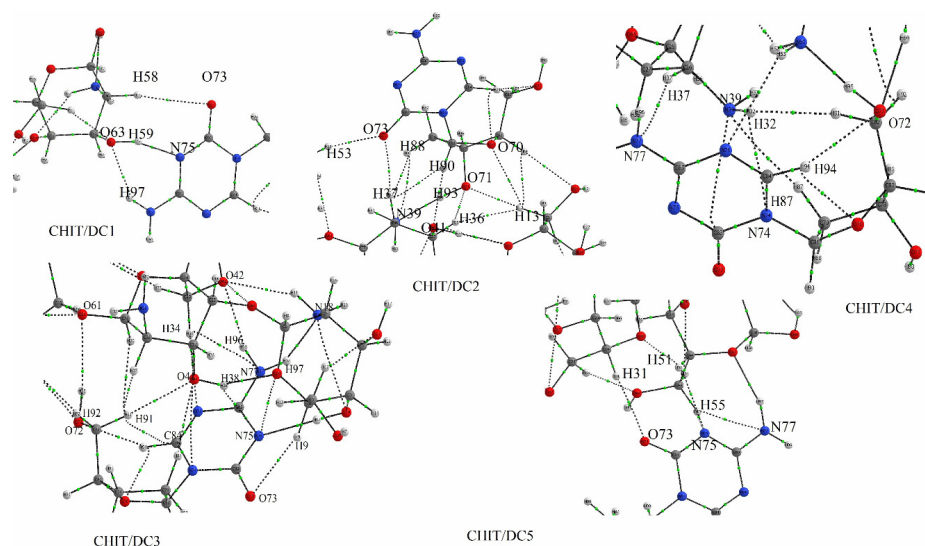


Figure 4: Molecular graph of CHIT/DC1-5; small green spheres and dotted lines relate to the bond critical points (BCP) and the bond paths, respectively

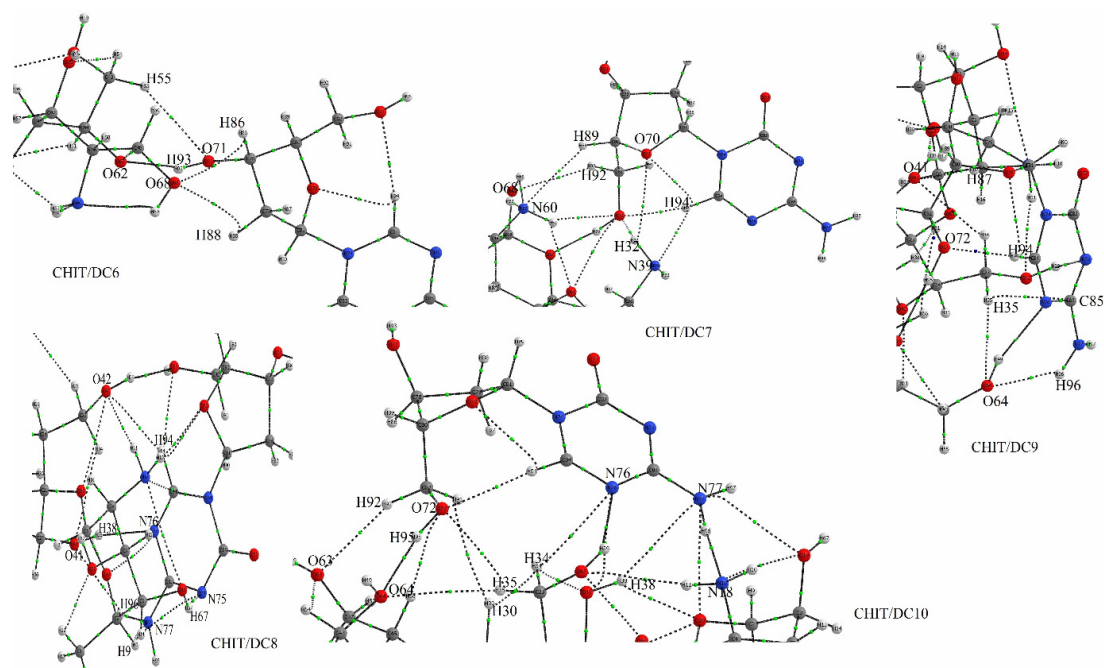


Figure 5: Molecular graph of CHIT/DC6-10; small green spheres and dotted lines relate to the bond critical points (BCP) and the bond paths, respectively

In the structures, we face two forms of hydrogen bonds, *i.e.*, O-H and N-H. We started with the most stable species (CHIT/DC10), where the NH_2 and N functional groups of DC approach the NH_2 and OH functional groups of CHIT, respectively. The $\text{H96}\cdots\text{N18}$ ($E_{\text{HB}} = -31.3 \text{ kJ/mol}^{-1}$) and $\text{H95}\cdots\text{O64}$ ($E_{\text{HB}} = -30.8 \text{ kJ/mol}^{-1}$) connections with $\nabla^2\rho > 0$, $H_b < 0$, $0.5 < -G_b/V_b < 1$ are medium hydrogen bonds, in which the first one ($\text{H96}\cdots\text{N18}$) with $-G_b/V_b = 0.9270$ is the strongest hydrogen bond in all the structures. The $\text{H56}\cdots\text{O72}$, $\text{H38}\cdots\text{N77}$, $\text{H37}\cdots\text{O72}$, $\text{H92}\cdots\text{O63}$, $\text{N76}\cdots\text{O41}$ and $\text{H34}\cdots\text{N76}$ interactions with $\nabla^2\rho > 0$, $H_b > 0$ and $-G_b/V_b > 1$ relate to weak hydrogen bonds. Because of this structure, the sum of the hydrogen bond energies ($\sum_{i=1}^8 E_{\text{HB}}^i$) is $-109.7 \text{ kJ/mol}^{-1}$. In addition to the bond critical points of the hydrogen bonds, there are two other interactions between oxygen and nitrogen (N77-O19 and N77-O20), as seen in Figure 5 (CHIT/DC10).

In CHIT/DC3, the second most stable configuration ($\sum_{i=1}^8 E_{\text{HB}}^i = -118.9 \text{ kJ/mol}^{-1}$) N and NH_2 functional groups of DC approach the

OH and O functional groups of CHIT. This structure provides medium hydrogen bonds, the most powerful of which is the $\text{H97}\cdots\text{N18}$ ($E_{\text{HB}} = -34.3 \text{ kJ/mol}^{-1}$). Three additional interactions ($\text{H34}\cdots\text{N77}$, $\text{H18}\cdots\text{O19}$, $\text{H96}\cdots\text{O42}$, $\text{H92}\cdots\text{O61}$ and $\text{H94}\cdots\text{O72}$) will be classified as weak hydrogen bonds. One of them is related to O-H interaction.

The third most stable species will be CHIT/DC2 ($\sum_{i=1}^8 E_{\text{HB}}^i = -111.2 \text{ kJ/mol}^{-1}$), where the OH and CO functional groups of DC connect to the CH_2OH and NH_2 functional groups of CHIT, respectively. In this particular structure, three medium hydrogen bonds are distinguished. CHIT/DC1 ($\sum_{i=1}^8 E_{\text{HB}}^i = -63.3 \text{ kJ/mol}^{-1}$) has two medium and one weak hydrogen bond. Within it, the NH_2 functional groups of DC connect to the CH_2OH functional groups of CHIT.

We actually found that CHIT/DC8 ($\sum_{i=1}^8 E_{\text{HB}}^i = -85.9 \text{ kJ/mol}^{-1}$), includes 1 medium hydrogen bond ($\text{H38}\cdots\text{N76}$) with $E_{\text{HB}} = -34.9 \text{ kJ/mol}^{-1}$, where the NH_2 functional group of DC approaches the OH functional group of CHIT.

Table 2
Topological parameters in a.u. and hydrogen bond energy (E_{HB}) in kJ mol⁻¹ for CHIT/DC1-10 at M06-2X/6-31G** level of theory

Atoms	$\rho(r)$	$\nabla^2\rho(r)$	G_b	V_b	H_b	$-G_b/V_b$	E_{HB}
CHIT/DC1							
H58 - O73	0.0070	0.0226	0.0050	-0.0044	0.0006	1.1388	-5.8
H59 - N75	0.0399	0.1018	0.0275	-0.0296	-0.0021	0.9300	-38.8
O63 - H97	0.0175	0.0543	0.0139	-0.0143	-0.0003	0.9765	-18.7
CHIT/DC2							
H37 - O73	0.0098	0.0307	0.0073	-0.0069	0.0004	1.0573	-9.0
H13 - O70	0.0073	0.0288	0.0062	-0.0053	0.0010	1.1852	-6.9
O41 - H90	0.0131	0.0388	0.0099	-0.0100	-0.0002	0.9828	-13.2
H13 - O71	0.0106	0.0326	0.0079	-0.0076	0.0003	1.0363	-10.0
H36 - O71	0.0115	0.0368	0.0087	-0.0082	0.0005	1.0604	-10.8
N39 - H93	0.0364	0.0852	0.0233	-0.0253	-0.0020	0.9211	-33.2
H53 - O73	0.0185	0.0593	0.0151	-0.0153	-0.0002	0.9846	-20.1
N39 - H88	0.0094	0.0316	0.0070	-0.0061	0.0009	1.1471	-8.0
CHIT/DC3							
H34 - N77	0.0078	0.0312	0.0064	-0.0050	0.0014	1.2800	-6.6
O42 - H96	0.0162	0.0549	0.0137	-0.0136	0.0001	1.0047	-17.8
N18 - H97	0.0362	0.0897	0.0243	-0.0262	-0.0019	0.9275	-34.4
O61 - H92	0.0047	0.0181	0.0036	-0.0028	0.0009	1.3211	-3.6
H38 - N75	0.0101	0.0373	0.0082	-0.0071	0.0011	1.1535	-9.3
H9 - O73	0.0089	0.0275	0.0064	-0.0060	0.0004	1.0738	-7.9
C84 - H91	0.0078	0.0314	0.0060	-0.0042	0.0018	1.4270	-5.6
O72 - H94	0.0127	0.0415	0.0100	-0.0096	0.0004	1.0387	-12.6
O41 - H91	0.0122	0.0368	0.0092	-0.0092	0.0000	1.0029	-12.0
O41 - H87	0.0100	0.0312	0.0074	-0.0069	0.0004	1.0616	-9.1
CHIT/DC4							
H37 - N77	0.0083	0.0250	0.0056	-0.0049	0.0007	1.1441	-6.4
H32 - N74	0.0086	0.0314	0.0067	-0.0057	0.0011	1.1941	-7.4
O72 - H94	0.0138	0.0448	0.0109	-0.0106	0.0003	1.0298	-13.8
N39 - H87	0.0092	0.0288	0.0065	-0.0058	0.0007	1.1244	-7.6
CHIT/DC5							
H31 - O73	0.0087	0.0297	0.0067	-0.0060	0.0007	1.1242	-7.8
H55 - N77	0.0060	0.0197	0.0042	-0.0035	0.0007	1.1988	-4.6
H55 - N75	0.0063	0.0211	0.0045	-0.0037	0.0008	1.2148	-4.8
H51 - N75	0.0111	0.0342	0.0077	-0.0068	0.0009	1.1329	-8.9
CHIT/DC6							
H55 - O71	0.0082	0.0277	0.0062	-0.0054	0.0008	1.1413	-7.1
O62 - H93	0.0319	0.0990	0.0253	-0.0259	-0.0005	0.9788	-33.9
O68 - H86	0.0077	0.0302	0.0063	-0.0051	0.0012	1.2384	-6.7
O68 - H88	0.0079	0.0307	0.0064	-0.0052	0.0013	1.2418	-6.8
CHIT/DC7							
H32 - O70	0.0056	0.0246	0.0050	-0.0039	0.0011	1.2879	-5.1
N39 - H94	0.0086	0.0363	0.0073	-0.0055	0.0018	1.3270	-7.2
O68 - H92	0.0084	0.0300	0.0065	-0.0054	0.0010	1.1909	-7.1
N60 - H89	0.0083	0.0256	0.0056	-0.0049	0.0008	1.1531	-6.4
CHIT/DC8							
O41 - H96	0.0121	0.0410	0.0099	-0.0095	0.0004	1.0413	-12.4
H9 - N77	0.0073	0.0239	0.0052	-0.0045	0.0007	1.1665	-5.9
H9 - N75	0.0058	0.0196	0.0041	-0.0033	0.0008	1.2384	-4.3
H38 - N76	0.0357	0.0986	0.0256	-0.0266	-0.0010	0.9637	-34.9
H67 - N75	0.0175	0.0541	0.0133	-0.0131	0.0002	1.0157	-17.2
O42 - H94	0.0115	0.0382	0.0091	-0.0086	0.0005	1.0582	-11.2
H9 - N77	0.0073	0.0239	0.0052	-0.0045	0.0007	1.1665	-5.9
H9 - N75	0.0058	0.0196	0.0041	-0.0033	0.0008	1.2384	-4.3

H38 - N76	0.0357	0.0986	0.0256	-0.0266	-0.0010	0.9637	-34.9
H67 - N75	0.0175	0.0541	0.0133	-0.0131	0.0002	1.0157	-17.2
O42 - H94	0.0115	0.0382	0.0091	-0.0086	0.0005	1.0582	-11.2
CHIT/DC9							
O64 - H96	0.0173	0.0592	0.0147	-0.0146	0.0001	1.0071	-19.1
H35 - C85	0.0105	0.0408	0.0083	-0.0064	0.0019	1.2909	-8.4
O72 - H94	0.0191	0.0555	0.0147	-0.0155	-0.0008	0.9471	-20.3
O41 - H87	0.0119	0.0392	0.0094	-0.0089	0.0004	1.0483	-11.7
CHIT/DC10							
N18 - H96	0.0345	0.0814	0.0221	-0.0238	-0.0017	0.9270	-31.3
H38 - N77	0.0045	0.0177	0.0036	-0.0028	0.0008	1.3021	-3.6
H34 - N76	0.0094	0.0344	0.0074	-0.0063	0.0012	1.1855	-8.2
H56 - O72	0.0098	0.0368	0.0080	-0.0067	0.0012	1.1839	-8.8
O63 - H92	0.0114	0.0338	0.0083	-0.0082	0.0001	1.0165	-10.7
H35 - O72	0.0095	0.0358	0.0077	-0.0065	0.0012	1.1849	-8.6
O64 - H95	0.0294	0.0925	0.0233	-0.0235	-0.0002	0.9920	-30.8

Table3
Quantum molecular descriptors (eV) for optimized geometries

Species	E _{HOMO}	E _{LUMO}	E _g	η	ω	Species	E _{HOMO}	E _{LUMO}	E _g	η	ω
B3LYP-H ₂ O						M06-2X-H ₂ O					
DC	-6.94	-0.98	5.96	2.98	2.63	DC	-8.53	0.09	8.63	4.31	2.07
CHIT	-6.41	1.49	7.90	3.95	0.77	CHIT	-8.16	2.69	10.85	5.42	0.69
CHIT/DC1	-6.41	-1.20	5.21	2.60	2.78	CHIT/DC1	-8.18	-0.14	8.04	4.02	2.15
CHIT/DC2	-6.46	-1.05	5.41	2.70	2.61	CHIT/DC2	-8.22	0.02	8.24	4.12	2.04
CHIT/DC3	-6.54	-1.04	5.51	2.75	2.61	CHIT/DC3	-8.22	0.04	8.26	4.13	2.03
CHIT/DC4	-6.41	-0.99	5.42	2.71	2.53	CHIT/DC4	-8.19	-0.11	8.08	4.04	2.13
CHIT/DC5	-6.40	-0.91	5.49	2.75	2.43	CHIT/DC5	-8.18	0.14	8.32	4.16	1.94
CHIT/DC6	-6.42	-0.95	5.47	2.73	2.49	CHIT/DC6	-8.19	0.12	8.32	4.16	1.96
CHIT/DC7	-6.45	-1.21	5.25	2.62	2.80	CHIT/DC7	-8.19	0.11	8.30	4.15	1.97
CHIT/DC8	-6.20	-0.87	5.33	2.66	2.34	CHIT/DC8	-8.02	0.11	8.13	4.06	1.92
CHIT/DC9	-6.51	1.18	5.33	2.67	2.77	CHIT/DC9	-8.22	-0.27	7.95	3.97	2.26
CHIT/DC10	-6.53	-0.95	5.58	2.79	2.51	CHIT/DC10	-8.19	0.11	8.31	4.15	1.97
B3LYP-GAS						M06-2X-GAS					
DC	-6.61	-0.77	5.84	2.92	2.34	DC	-8.20	0.30	8.50	4.25	1.83
CHIT	-6.02	1.35	7.37	3.69	0.74	CHIT	-7.97	2.60	10.39	5.19	0.65
CHIT/DC1	-5.96	-1.22	4.74	2.37	2.72	CHIT/DC1	-7.68	-0.14	7.54	3.77	2.03
CHIT/DC2	-6.06	-0.91	5.15	2.57	2.36	CHIT/DC2	-7.75	0.19	7.94	3.97	1.80
CHIT/DC3	-6.20	-0.61	5.59	2.80	2.07	CHIT/DC3	-7.96	0.32	8.28	4.14	1.77
CHIT/DC4	-6.12	-0.81	5.31	2.66	2.26	CHIT/DC4	-8.08	0.08	8.16	4.08	1.96
CHIT/DC5	-5.60	-0.63	4.97	2.48	1.95	CHIT/DC5	-7.79	0.66	8.45	4.23	1.50
CHIT/DC6	-5.80	-0.77	5.03	2.51	2.15	CHIT/DC6	-7.81	0.62	8.43	4.21	1.53
CHIT/DC7	-6.06	-1.02	5.05	2.52	2.48	CHIT/DC7	-7.73	0.57	8.30	4.15	1.55
CHIT/DC8	-5.87	-0.82	5.04	2.52	2.22	CHIT/DC8	-7.65	0.39	8.05	4.02	1.64
CHIT/DC9	-6.14	-1.10	5.05	3.52	2.60	CHIT/DC9	-7.91	-0.01	7.90	3.95	1.98
CHIT/DC10	-6.19	-0.46	5.73	2.86	1.93	CHIT/DC10	-8.03	0.31	8.33	4.17	1.79

Similar states are found for CHIT/DC9 and CHIT/DC6 ($\sum_{i=1}^8 E_{HB}^i = -59.5 \text{ kJ/mol}^{-1}$), $\sum_{i=1}^8 E_{HB}^i = -54.5 \text{ mol}^{-1}$, where the OH and N functional groups of DC connect to OH and NH₂ functional groups of CHIT, respectively. Probably the most unstable structure relates to CHIT/DC5 ($\sum_{i=1}^8 E_{HB}^i = -26.1 \text{ kJ/mol}^{-1}$), where the NH₂ functional group of DC approaches the CH₂OH

functional group of CHIT. The configuration has 4 weak interactions, 3 of which are related to N-H interactions (H55...N77, H55...N75 and H51...N75).

In Table 3, quantum molecular descriptors (electrophilicity power (ω) and global hardness (η)) and E_g gap of energy between LUMO (lowest unoccupied molecular orbital) and HOMO

(highest occupied molecular orbital) for DC, CHIT and CHIT/DC1-10, at M06-2X and B3LYP levels, are described (in both phases).

Considering Table 3, E_g and η of DC and CHIT/DC1-10 are almost identical. The parameters decreased in CHIT/DC1-10 structures. However, there is absolutely no considerable charge transfer between DC and CHIT. This is perfect for a drug delivery system, because the DC drug could be easily released from the exterior surface of this CHIT carrier. E_g and η values of CHIT/DC10 and CHIT/DC3 in aqueous solution are larger compared to those of other structures, which demonstrates that they are more stable than other structures. Because ω can be used to predict toxicity, it might be assumed that the toxicity of DC in the presence of CHIT will on average decrease.

CONCLUSION

Ten configurations of the non-bonded interactions of decitabine drug (DC) with chitosan (CHIT) nanocarrier were studied at B3LYP and M06-2X density functional levels in aqueous solution and gas phase (CHIT/DC1-10). The negative values of the binding energies demonstrated that the functionalization of CHIT with DC is energetically suitable. Solvation energies displayed that the solubility of DC increases in the presence of CHIT. Considering the electrophilicity power, the HOMO-LUMO energy gap and the global hardness, it may be assumed that the toxicity of DC in CHIT/DC1-10 will be reduced to some extent and its reactivity will increase. In addition, as shown by the AIM studies, the non-covalent adsorption of the drug on the carrier is mainly related to the hydrogen bonds. According to the AIM results, stronger and more hydrogen bonds exist in the most stable configuration (CHIT/DC10), where the NH_2 and N functional groups of DC interacts with the NH_2 and OH functional groups of CHIT, in the respective order.

ACKNOWLEDGEMENTS: We thank the Research Center for Animal Development Applied Biology for allocation of computer time.

REFERENCES

¹ D. S. Spencer, A. S. Puranik and N. A. Peppas, *Curr. Opin. Chem. Eng.*, **7**, 84 (2015), <https://doi.org/10.1016/j.coche.2014.12.003>

- ² M. Kamel, H. Raissi, A. Morsali and M. Shahabi, *Appl. Surf. Sci.*, **434**, 492 (2018), <https://doi.org/10.1016/j.apsusc.2017.10.165>
- ³ M. Lotfi, A. Morsali and M. R. Bozorgmehr, *Appl. Surf. Sci.*, **462**, 720 (2018), <https://doi.org/10.17586/2220-8054-2019-10-4-438-446>
- ⁴ S. Hamedani, S. Moradi and H. Aghaie, *Chinese J. Struct. Chem.*, **34**, 1161 (2015), <http://doi.org/10.13005/ojc/330309>
- ⁵ A. Chauhan, *Molecules*, **23**, 938 (2018), <https://doi.org/10.3390/molecules23040938>
- ⁶ B. S. Pattni, V. V. Chupin and V. P. Torchilin, *Chem. Rev.*, **115**, 10938 (2015), <https://doi.org/10.1021/acs.chemrev.5b00046>
- ⁷ N. Marasini, S. Haque and L. M. Kaminskas, *Curr. Opin. Colloid Interface Sci.*, **31**, 18 (2017), <https://doi.org/10.1016/j.cocis.2017.06.003>
- ⁸ K. Raza, N. Thotakura, P. Kumar, M. Joshi, S. Bhushan *et al.*, *Int. J. Pharm.*, **495**, 551 (2015), <https://doi.org/10.1016/j.ijpharm.2015.09.016>
- ⁹ S. K. Shukla, A. K. Mishra, O. A. Arotiba and B. B. Mamba, *Int. J. Biol. Macromol.*, **59**, 46 (2013), <https://doi.org/10.1016/j.ijbiomac.2013.04.043>
- ¹⁰ A. Ali and S. Ahmed, *Int. J. Biol. Macromol.*, **109**, 273 (2018), <https://doi.org/10.1016/j.ijbiomac.2017.12.078>
- ¹¹ H. S. Adhikari and P. N. Yadav, *Int. J. Biomater.*, **2018**, 2952085 (2018), <https://doi.org/10.1155/2018/2952085>
- ¹² R. Shanmuganathan, T. N. J. I. Edison, F. L. Oscar and K. Ponnuchan, *Int. J. Biol. Macromol.*, **130**, 727 (2019), <https://doi.org/10.1016/j.ijbiomac.2019.02.060>
- ¹³ R. Nicu, E. Bobu and J. Desbrieres, *Cellulose Chem. Technol.*, **45**, 105 (2011), [https://www.cellulosechemtechnol.ro/pdf/CCT1-2\(2011\)/p.105-111.pdf](https://www.cellulosechemtechnol.ro/pdf/CCT1-2(2011)/p.105-111.pdf)
- ¹⁴ M. Wu, W. Lv, F. Wang, Z. Long, J. Chen *et al.*, *Cellulose Chem. Technol.*, **52**, 43 (2018), [https://www.cellulosechemtechnol.ro/pdf/CCT1-2\(2018\)/p.43-49.pdf](https://www.cellulosechemtechnol.ro/pdf/CCT1-2(2018)/p.43-49.pdf)
- ¹⁵ A. Kumari, S. K. Yadav, Y. B. Pakade and B. Singh, *Colloids Surf. B*, **80**, 184 (2010), <https://doi.org/10.1016/j.colsurfb.2010.06.002>
- ¹⁶ L. Andze, J. Zoldners, L. Rozenberga, I. Sable, M. Skute *et al.*, *Cellulose Chem. Technol.*, **52**, 873 (2018), [https://www.cellulosechemtechnol.ro/pdf/CCT9-10\(2018\)/p.873-881.pdf](https://www.cellulosechemtechnol.ro/pdf/CCT9-10(2018)/p.873-881.pdf)
- ¹⁷ F. Akman, *Cellulose Chem. Technol.*, **51**, 253 (2017), [https://www.cellulosechemtechnol.ro/pdf/CCT3-4\(2017\)/p.253-262.pdf](https://www.cellulosechemtechnol.ro/pdf/CCT3-4(2017)/p.253-262.pdf)
- ¹⁸ X.-F. Zheng, Q. Lian, H. Yang and X. Wang, *Sci. Rep.*, **6**, 21409 (2016), <https://doi.org/10.1038/srep21409>
- ¹⁹ P. Li, Y. Wang, Z. Peng, F. She and L. Kong, *Carbohydr. Polym.*, **85**, 698 (2011), <https://doi.org/10.1016/j.carbpol.2011.03.045>

- ²⁰ A. Nawaz and T. W. Wong, *J. Investig. Dermatol.*, **138**, 2412 (2018), <https://doi.org/10.1016/j.jid.2018.04.037>
- ²¹ H. Horo, S. Das, B. Mandal and L. M. Kundu, *Int. J. Biol. Macromol.*, **121**, 1070 (2019), <https://doi.org/10.1016/j.ijbiomac.2018.10.095>
- ²² K. Yoncheva, M. Merino, A. Shenol, N. T. Daskalov, P. S. Petkov *et al.*, *Int. J. Pharm.*, **556**, 1 (2019), <https://doi.org/10.1016/j.ijpharm.2018.11.070>
- ²³ A. Khdair, I. Hamad, H. Alkhatib, Y. Bustanji, M. Mohammad *et al.*, *Eur. J. Pharm. Sci.*, **93**, 38 (2016), <https://doi.org/10.1016/j.ejps.2016.07.012>
- ²⁴ A. V. Nascimento, A. Singh, H. Bousbaa, D. Ferreira, B. Sarmiento *et al.*, *Acta Biomater.*, **47**, 71 (2017), <https://doi.org/10.22034/nmrj.2017.62889.1065>
- ²⁵ M. Moura, M. Gil and M. Figueiredo, *Eur. Polym. J.*, **49**, 2504 (2013), <https://doi.org/10.1021/bm200731x>
- ²⁶ A. Portero, C. Remunan-Lopez and J. Vila-Jato, *Int. J. Pharm.*, **175**, 75 (1998), <https://doi.org/10.1007/s13233-010-1004-0>
- ²⁷ N. T. Chinh, N. T. T. Trang, N. V. Giang, D. T. M. Thanh, T. T. X. Hang *et al.*, *J. Appl. Polym. Sci.*, **133** (2016), <https://doi.org/10.1007/s10924-020-01727-6>
- ²⁸ L. P. Jahromi, F. M. Panah, A. Azadi and H. Ashrafi, *Int. J. Biol. Macromol.*, **125**, 785 (2019), <https://doi.org/10.3390/biomedicines8010013>
- ²⁹ A. Alexander, S. Saraf and S. Saraf, *Drug Dev. Ind. Pharm.*, **41**, 1954 (2015), <https://doi.org/10.3109/03639045.2015.1011167>
- ³⁰ M. Nag, V. Gajbhiye, P. Kesharwani and N. K. Jain, *Colloids Surf. B*, **148**, 363 (2016), <https://doi.org/10.1016/j.colsurfb.2016.08.059>
- ³¹ E. Lee, J. Lee, I.-H. Lee, M. Yu, H. Kim *et al.*, *J. Med. Chem.*, **51**, 6442 (2008), <https://doi.org/10.1021/jm800767c>
- ³² S. Natesan, C. Ponnusamy, A. Sugumaran, S. Chelladurai, S. S. Palaniappan *et al.*, *Int. J. Biol. Macromol.*, **104**, 1853 (2017), <https://doi.org/10.1016/j.ijbiomac.2017.03.137>
- ³³ J.-B. Qu, H.-H. Shao, G.-L. Jing and F. Huang, *Colloids Surf. B*, **102**, 37 (2013), <https://doi.org/10.1016/j.colsurfb.2012.08.004>
- ³⁴ S. A. Agnihotri and T. M. Aminabhavi, *Int. J. Pharm.*, **324**, 103 (2006), <https://doi.org/10.1016/j.ijpharm.2006.05.061>
- ³⁵ R. Mo, Y. Xiao, M. Sun, C. Zhang and Q. Ping, *Int. J. Pharm.*, **409**, 38 (2011), <https://doi.org/10.1016/j.ijpharm.2011.02.021>
- ³⁶ G. Arya, M. Vandana, S. Acharya and S. K. Sahoo, *Nanomedicine*, **7**, 859 (2011), <https://doi.org/10.1016/j.nano.2011.03.009>
- ³⁷ W. J. Trickler, J. Khurana, A. A. Nagvekar and A. K. Dash, *Aaps. Pharm. Sci. Tech.*, **11**, 392 (2010), <https://doi.org/10.1208/s12249-010-9393-0>
- ³⁸ H. Zheng, Y. Rao, Y. Yin, X. Xiong, P. Xu *et al.*, *Carbohydr. Polym.*, **83**, 1952 (2011), <https://doi.org/10.1016/j.carbpol.2010.10.069>
- ³⁹ Y. S. Elnaggar, S. M. Etman, D. A. Abdelmonsif and O. Y. Abdallah, *J. Pharm. Sci.*, **104**, 3544 (2015), <https://doi.org/10.1002/jps.24557>
- ⁴⁰ A. Dev, N. Binulal, A. Anitha, S. Nair, T. Furuike *et al.*, *Carbohydr. Polym.*, **80**, 833 (2010), <https://doi.org/10.1016/j.carbpol.2009.12.040>
- ⁴¹ S. Kamalzare, Z. Noormohammadi, P. Rahimi, F. Atyabi, S. Irani *et al.*, *J. Cell. Physiol.*, **234**, 20554 (2019), <https://doi.org/10.1002/jcp.28655>
- ⁴² W. Kunanusornchai, B. Witoonpanich, T. Tawonsawatruk, R. Pichyangkura, V. Chatsudthipong *et al.*, *Pharmacol. Res.*, **113**, 458 (2016), <https://doi.org/10.1016/j.phrs.2016.09.016>
- ⁴³ S. Li, S. Cui, D. Yin, Q. Zhu, Y. Ma *et al.*, *Nanoscale*, **9**, 3912 (2017), <https://doi.org/10.1039/C6NR07188K>
- ⁴⁴ N. Saikia and R. C. Deka, *J. Struct. Chem.*, **25**, 593 (2014), <https://doi.org/10.1007/s11224-013-0327-9>
- ⁴⁵ H. Chegini, A. Morsali, M. Bozorgmehr and S. Beyramabadi, *Prog. React. Kinet. Mec.*, **41**, 345 (2016), <http://dx.doi.org/10.13005/ojpc/310318>
- ⁴⁶ H. Xu, L. Li, G. Fan and X. Chu, *Comput. Theor. Chem.*, **1131**, 57 (2018), <https://doi.org/10.1016/j.comptc.2018.03.032>
- ⁴⁷ H. Lari, A. Morsali and M. M. Heravi, *Nanosystems: Physics, Chemistry, Mathematics*, **10**, 438 (2019), <https://doi.org/10.17586/2220-8054-2020-11-3-285-293>
- ⁴⁸ M. Frisch, G. Trucks, H. Schlegel, G. Scuseria, M. Robb *et al.*, Gaussian 09, revision B.01. Gaussian, Inc., Wallingford, CT (2009), <https://gaussian.com>
- ⁴⁹ Y. Zhao and D. G. Truhlar, *Theor. Chem. Acc.*, **120**, 215 (2008), <https://doi.org/10.1007/s00214-007-0310-x>
- ⁵⁰ J. D. Dill and J. A. Pople, *J. Chem. Phys.*, **62**, 2921 (1975), <https://doi.org/10.1063/1.430801>
- ⁵¹ A.D. Becke, *J. Chem. Phys.*, **98**, 5648 (1993), <https://doi.org/10.1007/s002149900065>
- ⁵² J. Tomasi and M. Persico, *Chem. Rev.*, **94**, 2027 (1994), <https://doi.org/10.1021/cr00031a013>
- ⁵³ E. L. Coitiño, J. Tomasi and R. Cammi, *J. Comput. Chem.*, **16**, 20 (1995), <https://doi.org/10.1002/jcc.540160103>
- ⁵⁴ R. G. Parr, L. V. Szentpaly and S. Liu, *J. Am. Chem. Soc.*, **121**, 1922 (1999), <https://doi.org/10.1021/ja983494x>
- ⁵⁵ T. A. Keith and T. K. Gristmill, Software, Overland Park KS, USA (2013), <http://aim.tkgristmill.com>
- ⁵⁶ R. F. Bader, *Chem. Rev.*, **91**, 893 (1991), <https://doi.org/10.1021/cr00005a013>
- ⁵⁷ Y. Zhao and D. G. Truhlar, *Theor. Chem. Acc.*, **120**, 215 (2008), <https://doi.org/10.1063/1.2912068>
- ⁵⁸ B. C. Deka and P. K. Bhattacharyya, *Comput. Theor. Chem.*, **1110**, 40 (2017), <https://doi.org/10.1016/j.comptc.2017.03.036>
- ⁵⁹ B. C. Deka and P. K. Bhattacharyya, *Comput. Theor. Chem.*, **1051**, 35 (2015), <https://doi.org/10.1016/j.comptc.2014.10.023>

⁶⁰ M. Nasrabadi, S. A. Beyramabadi and A. Morsali, *Int. J. Biol. Macromol.*, **147**, 534 (2020), <https://doi.org/10.1016/j.ijbiomac.2020.01.070>

⁶¹ P. Geetha, A. J. Sivaram, R. Jayakumar and C. G. Mohan, *Carbohydr. Polym.*, **142**, 240 (2016), <https://doi.org/10.1016/j.carbpol.2016.01.059>

⁶² S.-H. Lin, W. Cui, G.-L. Wang, S. Meng, Y.-C. Liu *et al.*, *Drug Des. Devel. Ther.*, **10**, 2973 (2016), <https://doi.org/10.2147/DDDT.S114663>

⁶³ F. Naghavi, A. Morsali and M. R. Bozorgmehr, *J. Mol. Liq.*, **282**, 392 (2019), <https://doi.org/10.1016/j.molliq.2019.03.040>

⁶⁴ I. Rozas, I. Alkorta and J. Elguero, *J. Am. Chem. Soc.*, **122**, 11154 (2000), <https://doi.org/10.1021/ja0017864>